Iterated Correlation Under Uncertainty: A Three-Layer Predictive Model with Fuzzy Upper Bounds

ALHAJJ HASSAN Ishrak[1]

[1] *University of Ostrava*
Ostrava, Czech Republic
E-mail: Ishrak.Alhajj.s01@osu.cz

The early applications of iterated correlations for clustering and block-modeling go back to psychometrics and social networks [4, 6], with later visualization work through successive correlation sharpening [5]. We study the discrete dynamical system obtained by iterating the correlation operator. Starting from a real matrix $P_0 \in \mathbb{R}^{n\times n}$ with entries drawn i.i.d. from $U[-1,1]$, one step applies Pearson row–row correlation across the n columns to form

$$\big[P_{k+1}\big]_{ij} = \frac{\sum_{\ell=1}^{n}\big((P_k)_{i\ell}-\bar{p}_i\big)\big((P_k)_{j\ell}-\bar{p}_j\big)}{\sqrt{\sum_{\ell=1}^{n}\big((P_k)_{i\ell}-\bar{p}_i\big)^2}\,\sqrt{\sum_{\ell=1}^{n}\big((P_k)_{j\ell}-\bar{p}_j\big)^2}},$$

where $\bar{p}_i$ is the mean of the row i. Computation is repeated until element-wise entries stabilize with tolerance 10^{-12}:

$$\max_{i,j}\big|(P_{k+1})_{ij}-(P_k)_{ij}\big| \le 10^{-12}.$$

We ran 10^3 trials per size n in the set

$$\{3,6,7,9,12,16,23,30,40,50,55,69,80,100,150,250,350,600,1054,1600,1700,2000\},$$

and for each run we recorded the trajectory and the stepwise quantities

$$\Delta_k := \|P_{k+1}-P_k\|_F, \qquad \rho_k := \frac{\Delta_{k+1}}{\Delta_k}.$$

Goal. This study characterizes the dynamics of the iterated correlation, identifying four empirical laws that remain stable across matrix sizes and random initializations. The sequence (P_k) exhibits a dimension-independent contraction geometry that enables systematic stepwise prediction. Building on this structure, we develop a three-layer uncertainty-aware framework that remains reliable under sampling noise, compounding uncertainty, and decision imprecision.

1. **Universal first-step contraction:** The initial ratio $\rho_0 = \Delta_1/\Delta_0$ is uniformly small ($\rho_0 \ll 1$), producing a sharp, dimension-independent early drop in Δ_k.

2. **Nearly monotone convergence:** For $k \ge 1$, Δ_k decays almost monotonically; $\rho_k \approx 1$ with bounded, vanishing oscillations; occasional overshoots ($\rho_k > 1$) are uniformly bounded.

3. **Uniformly bounded iteration counts:** The number of steps to reach a fixed tolerance ($\Delta_k < 10^{-12}$) remains in a tight band across all tested n, suggesting $T(n,\varepsilon) = O(1)$ empirically.

Acknowledgement This work was supported by the University of Ostrava.

https://www.doi.org/10.15452/978-80-7599-515-5.2026.01

4. **Universal V-shape, dimension-independent contraction law:** Pooling (Δ_k, ρ_k) on log–log axes yields a single V-shaped curve: strong contraction for large Δ_k, a valley near $\Delta^\star$ ($\rho(\Delta^\star) \approx 10^{-2}$–$10^{-1}$), then a rise toward 1 as $\Delta_k \to 0$, with bounded right-branch overshoots resembling self-normalizing maps such as matrix scaling [7] and iterative normalization in deep networks [8], though the present operator is neither linear nor globally contractive.

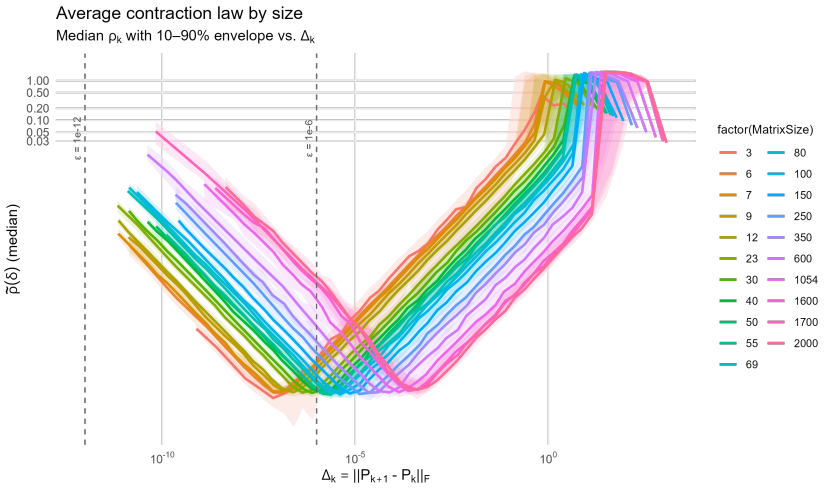

Figure 1: V-shape: median ribbons of ρ versus raw step size Δ (log–log) across matrix sizes n. The location of the valley $\Delta^\star$ and the bounded right-branch overshoot are consistent across sizes.

Geometric rationale and ongoing theoretical work. The four empirical laws arise from the geometry of the composite map $f = \Phi \circ \Psi$ defining the iteration $P_{k+1} = f(P_k)$, where Ψ performs row-centering, projecting onto the mean-zero hyperplane, and Φ applies normalization followed by a Gram lift. At large steps, Ψ acts as a strong projection, producing the sharp contraction that forms the left branch of the V-shape. Near equilibrium, Φ and Ψ nearly cancel along tangent directions, yielding almost distance-preserving updates (right branch). For the sequence $\{P_k\}_{k\geq 0}$, the cumulative total variation up to step K is

$$V_K := \sum_{k=0}^{K-1} \Delta_k,$$

which empirically converges to a finite limit $V_\infty \leq C$ with C independent of n. Since $V_\infty < \infty$ implies $\Delta_k \to 0$, the flow $P_{k+1} = f(P_k)$ stabilizes in $O(1)$ steps, uniformly in n. A theoretical study via global descent and local geometric analysis is underway.

From geometry to predictive bounds. To translate this contraction geometry into a predictive framework, we first extract an empirical median response $g(\Delta)$ capturing the pattern of (Δ, ρ) across sizes. This baseline curve then serves as the foundation for three predictive layers: (i) a thin-tail upper q_p^{naive} addressing sampling variability; (ii) a tail-conservative inflation q_p^{TC} controlled by τ to capture compounding "error-on-error" uncertainty in the sense of [1]; and (iii) a fuzzy bound U_α introducing decision-level tolerance. Together, these yield a family of bounds parameterized by $(p, \tau, \alpha, \lambda)$ while preserving the geometry revealed in Figure 1.

Baseline. From (Δ_k, ρ_k) we drop the first two transitions, optionally normalize by n via $\delta_k = \Delta_k/n$, trim the 1%–99% tails of Δ, and bin Δ on a logarithmic grid $\{B_j\}_{j=1}^K$ with

centers Δ_j. Within each bin we work in the log-domain to stabilize multiplicative noise and then exponentiate back so that $g(\Delta)$, $\sigma(\Delta)$, and all predictive layers are expressed on the original ρ-scale:

$$m(\Delta_j) \;:=\; \text{median}\big(\log \rho \,\big|\, \Delta \in B_j\big), \qquad q_\gamma^{\log}(\Delta_j) \;:=\; \text{quantile}_\gamma\big(\log \rho \,\big|\, \Delta \in B_j\big).$$

The baseline median response is $g(\Delta) \;:=\; \exp\big(m(\Delta)\big)$, with compatible dispersion

$$\sigma(\Delta) \;:=\; \frac{\exp\big(q_\gamma^{\log}(\Delta)\big) - g(\Delta)}{z_\gamma}, \quad z_\gamma := \Phi_{\mathcal{N}}^{-1}(\gamma), \;\; \gamma = 0.90,$$

where γ is a fixed quantile level used only for estimating scale and z_γ is its associated standard-normal upper quantile.

Layer 1: Thin-Tail Predictive Upper. Here $p \in (0.5, 0.999)$ denotes a target right-tail probability and $z_p := \Phi_{\mathcal{N}}^{-1}(p)$ is the corresponding standard-normal upper quantile. We define the *thin-tail* predictive upper quantile for $\rho \mid \Delta$ by

$$q_p^{\text{naive}}(\Delta) \;:=\; g(\Delta) \;+\; \sigma(\Delta)\, z_p.$$

This construction respects the V-shaped median geometry via $g(\Delta)$ and adjusts for sampling variability through the local scale $\sigma(\Delta)$.

Layer 2: Tail-Conservative Inflation. Even stable bin-wise fits may *understate* uncertainty in the extreme right tail because model mis-specification compounds (*error-on-error*) across transformations, as emphasized in the regress-of-uncertainty argument of [1]. We model this compounding scale uncertainty by a multiplicative factor $E \sim \text{LogN}(0, \tau^2)$, where $\tau > 0$ controls the magnitude of this effect. A standard log-domain argument shows that compounding scale error yields the inflation

$$\text{infl}(\tau) \;:=\; \exp\Big(\tfrac{1}{2}\,\tau^2\Big),$$

and therefore the *tail-conservative* predictive upper

$$q_p^{\text{TC}}(\Delta) \;:=\; g(\Delta) \;+\; \sigma(\Delta)\,\text{infl}(\tau)\, z_p.$$

Here τ tunes the strength of the error-on-error correction without altering the learned V-shaped geometry encoded in $g(\Delta)$.

Layer 3: Fuzzy Bound. Let $\alpha \in [0, 1]$ be an *acceptance* level (higher α = tighter bound) and $\lambda > 0$ a width parameter. We model a dilation in the sense of fuzzy-set theory [2, 3] by the α-cut of a linear membership above q_p^{TC}, giving the fuzzy upper:

$$U_\alpha(\Delta) \;:=\; \big(1 + \lambda(1-\alpha)\big)\, q_p^{\text{TC}}(\Delta).$$

Here $U_1 = q_p^{\text{TC}}$ and $U_0 = (1+\lambda)\, q_p^{\text{TC}}$; varying α traces a family of admissible upper bounds consistent with a chosen tolerance.

Properties. For fixed (τ, λ), the maps $\Delta \mapsto q_p^{\text{naive}}(\Delta)$, $\Delta \mapsto q_p^{\text{TC}}(\Delta)$, and $\Delta \mapsto U_\alpha(\Delta)$ all refine the baseline $g(\Delta)$ in an order-preserving manner on the ρ-scale (each lies above g and respects its V-shaped geometry). They are monotone in both the right-tail probability p and the tolerance parameter $(1-\alpha)$, so increasing either produces a larger upper bound. They are

Replace σ by σE; at high p, for a standard normal Z one has $Q_p(\sigma E\, Z) \approx \sigma\, e^{\frac{1}{2}\tau^2} z_p$.

also scale-equivariant in Δ and portable across n: replacing Δ by $\delta = \Delta/n$ re-parameterizes but does not change the inherited dimension-independent shape of the median curve $g(\Delta)$.

Result. The three layers turn the universal V-shape into uncertainty-aware bounds. q_p^{naive} provides a reproducible predictive upper; q_p^{TC} adjusts for compounding error-on-error uncertainty in the spirit of [1]; and U_α introduces controllable tolerance through fuzzy dilation [2, 3]. Data determine the empirical geometry through $g(\Delta)$ and $\sigma(\Delta)$, while $(p, \tau, \alpha, \lambda)$ act as interpretable tuning parameters. This construction cleanly separates the geometry learned from the data from the user-controlled parameters that encode tolerance and caution. At representative scales, as shown in Figure 2, the three bounds preserve a strict ordering:

$$q_p^{\text{naive}}(\Delta) \;<\; q_p^{\text{TC}}(\Delta) \;<\; U_{0.9}(\Delta) \;<\; U_{0.5}(\Delta) \qquad \text{for all } p \in [0.80, 0.999],$$

confirming stability and controllable risk tolerance through p and α.

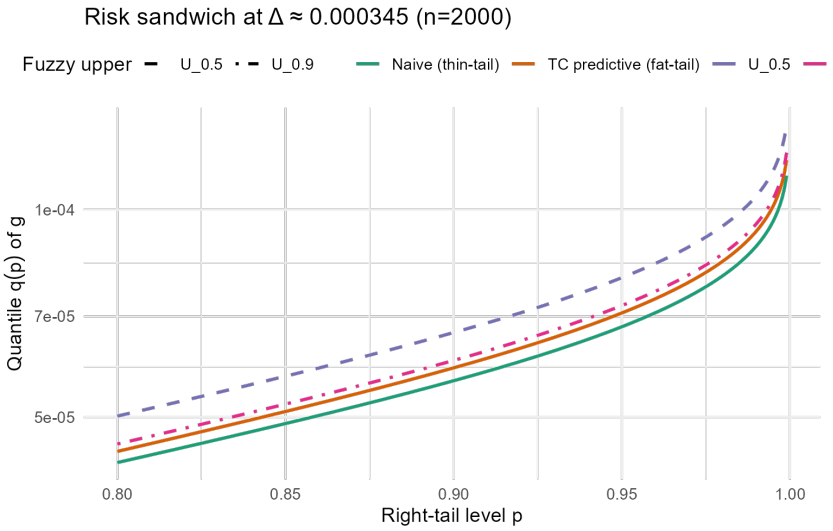

Figure 2: Layered bounds at a representative scale (75% step-size bin): thin-tail q_p^{naive}, tail-conservative q_p^{TC}, and fuzzy uppers $U_{0.5}, U_{0.9}$ traced over $p \in [0.80, 0.999]$.

Conclusion. The iterated correlation dynamics exhibit a dimension-independent V-shaped contraction arising from the finite-variation trajectory of (P_k). The three-layer framework translates this geometry into actionable predictive tools for real-world computation. Parameterized by $(p, \tau, \alpha, \lambda)$, the resulting bounds are reproducible, interpretable, and suitable for adaptive stopping, consistency checks, and control in normalization-driven or learning algorithms.

References

[1] N. N. Taleb and P. Cirillo: *The Regress of Uncertainty and the Forecasting Paradox.* SSRN Working Paper **5578812** (2025). URL: https://ssrn.com/abstract=5578812

[2] L. A. Zadeh: *Fuzzy Sets.* Information and Control **8** (1965) 338–353.

[3] V. Novák: *Perception-based Logical Deduction.* Springer (2012).

[4] L. L. McQuitty: *Multiple clustering revisited: Comments, comparisons, new approaches.* Multivariate Behavioral Research **3**(4) (1968) 431–479.

[5] C.-C. Chen, M. Yang, and C. Wu: *Generalized association plots: Information visualization via iteratively generated correlation matrices.* Statistica Sinica (2002). Journal homepage: http://www3.stat.sinica.edu.tw/statistica/

[6] R. L. Breiger, S. A. Boorman, and P. Arabie: *An algorithm for clustering relational data with applications to social network analysis and comparison with multidimensional scaling.* Journal of Mathematical Psychology **12**(3) (1975) 328–383.

[7] R. Sinkhorn: *A relationship between arbitrary positive matrices and doubly stochastic matrices.* The Annals of Mathematical Statistics (1964).

[8] L. Huang, D. Yang, and B. Lang: *Iterative normalization: Beyond standardization towards efficient whitening.* In: Proc. IEEE Conference on Computer Vision and Pattern Recognition (CVPR) (2019). OpenAccess: https://openaccess.thecvf.com/